Design and Integration of Electrical Bio-Impedance Sensing in a Bipolar Forceps for Soft Tissue Identification: A Feasibility Study

Chapter · February 2020

DOI: 10.1007/978-981-13-3498-6_1

5 authors, including:

Zhuoqi Cheng
Istituto Italiano di Tecnologia
16 PUBLICATIONS **138** CITATIONS
SEE PROFILE

Diego Dall'Alba
University of Verona
20 PUBLICATIONS **49** CITATIONS
SEE PROFILE

Paolo Fiorini
University of Verona
188 PUBLICATIONS **4,219** CITATIONS
SEE PROFILE

Design and integration of electrical bio-impedance sensing in a bipolar forceps for soft tissue identification: a feasibility study

Zhuoqi Cheng[1], Diego Dall'Alba[2], Darwin G. Caldwell[1], Paolo Fiorini[2] and Leonardo S. Mattos[1]

[1] Department of Advanced Robotics, Istituto Italiano di Tecnologia, Genova, Italy
[2] Department of Computer Science, University of Verona, Verona, Italy

Abstract— **This paper presents the integration of electrical bio-impedance sensing technology into a bipolar surgical forceps for soft tissue identification during a robotic assisted procedure. The EBI sensing is done by pressing the forceps on the target tissue with a controlled pressing depth and a controlled jaw opening distance. The impact of these 2 parameters are characterized by finite element simulation. Subsequently, an experiment is conducted with 4 types of ex-vivo tissues including liver, kidney, lung and muscle. The experimental results demonstrate that the proposed EBI sensing method can identify these 4 tissue types with an accuracy higher than 92.82%.**

Keywords— **electrical bio-impedance, tissue identification, bipolar forceps, electrode configuration, finite element method**

I. Introduction

Robot-assisted minimal invasive surgery (RMIS) has been increasingly adopted in the clinical setting in the last fifteen years since this technology provides many benefits for both patients and surgeons. From the patient side, RMIS guarantees better outcomes than other more invasive approaches (i.e. open-surgery), similar to other minimally invasive surgical procedures (e.g. laparoscopy) [1]. From the surgeons point of view, RMIS guarantees improved dexterity, movements scaling and magnified tri-dimensional video feedback. Unfortunately, RMIS technologies available nowadays suffer from the limitations in terms of sensing modalities. Vision from the endoscopic cameras is the only sensing method for most commercial surgical robots. Due to the intrinsic limitations of endoscopic video images, performing automatic detection of different tissue types based on this data source can not provide the required robustness and reliability for supporting the execution of surgical procedure, especially when the field of view is under poor illumination, partially occluded, or foggy due to surgical smoke [2].

Electrical bio-impedance (EBI) sensing has potential to be very helpful in this application, enabling reliable and robust tissue identification while providing advantages such as low cost and fast detection. For instance, EBI technology is able to identify different tissue types with a needle electrode, as shown in [3]. In [4, 5], Cheng *et al.* exploit the EBI sensor with a concentric electric needle to detect blood during a peripheral intravenous catheterization, showing a significant improvement of the operation success rate. In addition, different systems and techniques based on EBI sensing are proposed and developed for various cancer diagnosis such as hepatic cancer [6], breast cancer [7] and skin cancer [8].

Nevertheless, the capability and accuracy of tissue identification by measuring their EBI property significantly depends on the electrodes' configuration such as the relative distance and the size of electrodes [9]. Thus, most works in previous literature are based on custom designed EBI sensing probes that avoid this problem by imposing fixed electrode configuration. The adoption of the same solution in RMIS procedures is complex because it would require the design of a novel surgical tool with integrated EBI sensor or a drop-in probe.

In this study, we propose to simplify this issue by integrating the EBI sensing capability to existing robotic bipolar forceps. This requires minimum hardware modifications as the electrodes of the bipolar forceps can be readily used as the sensing electrodes. With the proposed system, the surgeon can perform real-time tissue identification by slightly pressing the forceps on the tissue surface, directly during the surgical tissue manipulation.

II. Methods

A. EBI sensing modeling

Fig.1 shows the modeling of EBI sensing using a bipolar forceps. Since this study focuses on soft tissues and the EBI measurement is done by touching the tissue producing a small pressing depth ($d \leq 4\,mm$), we assume that the induced tissue deformation ensures a complete contact between the electrode surface and the tissue. Electrode 1 and Electrode 2 are the two jaws of the bipolar forceps. To measure the EBI of the tissue, a safe electrical AC voltage (U) is injected. By obtaining the reciprocal current (I), the electrical impedance (Z) can be calculated as $Z = \frac{U}{I}$. Furthermore, the reciprocal current I can be obtained by integrating the current density J through a cross-sectional area A.

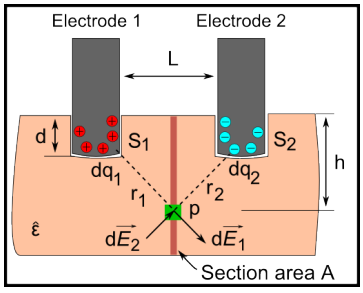

Fig. 1: Modeling the EBI sensing of soft tissue with a bipolar forceps.

$$I = \int_A J = \int_A (-i\omega\hat{\varepsilon}E) \tag{1}$$

Specifically, the current density J at a point p on the area A can be computed as the product of complex permittivity of the contacting tissue ($\hat{\varepsilon}$) and the electrical field strength E at that point. Also, the complex permittivity $\hat{\varepsilon}$ is a function of tissue conductivity σ, permittivity ε' and excitation frequency ω: $\hat{\varepsilon} = i\sigma/\omega + \varepsilon'$. Moreover, $|Z|$ can be computed as

$$|Z| = \frac{|U|}{|\omega\hat{\varepsilon}||\int_A E|} \tag{2}$$

Given that U has a constant amplitude, $|Z|$ depends on two variables: the electric field generated by the jaws of the forceps E and the electric properties of the contacting material $\hat{\varepsilon}$. Assuming the contacting material is homogeneous and a constant frequency ω is used, $|\omega\hat{\varepsilon}|$ is identical for each tissue type. Thus, we can assume that it is independent of the electric field strength E to simplify the model.

The electric field strength $\vec{E}$ is the sum of the electric field generated by Electrode 1 ($\vec{E_1}$) and Electrode 2 ($\vec{E_2}$), and they can be calculated using the Coulomb's law:

$$dE = dE_1 + dE_2 = \int_{S_1} \frac{dq_1}{4\pi\varepsilon_0 r_1^2} + \int_{S_2} \frac{dq_2}{4\pi\varepsilon_0 r_2^2} \tag{3}$$

where ε_0 is the electric constant, and S_1 and S_2 are the contacting area of Electrode 1 and 2 respectively, which are functions of the insertion depth d. r_i is the distance from a face element on Electrode i to Point p, and dq_i is the charge on the face element. In addition, r_i is a function of the electrode pressing depth d, the jaw opening distance L, and the depth of point h: $r_i = \sqrt{(h-d)^2 + (L/2)^2}$

Consequently, we can find that d and L are the two main parameters that impact the measurement of $|Z|$. To better characterize their influences, quantitative analysis is done by Finite Element (FE) simulation before testing the proposed EBI sensing method with ex-vivo tissue samples.

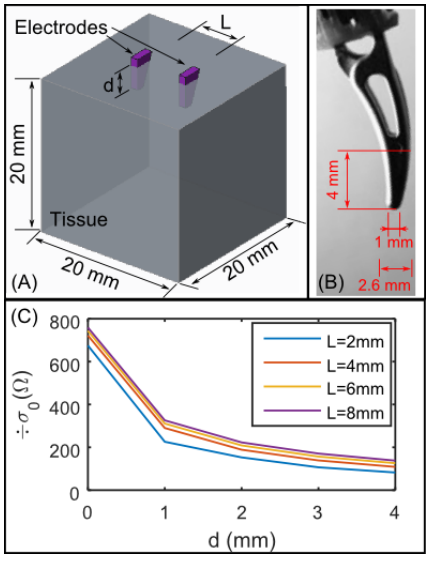

Fig. 2: (A) The FEM simulation of the EBI sensing with a bipolar forceps. (B) The dimension of the Maryland bipolar forceps. (C) The simulation results of EBI with different d and L.

B. FE Simulation of EBI sensing with a bipolar forceps

As shown in Fig. 2(A), the tissue is modelled as an homogeneous and isotropic gray block ($20\times20\times20\,mm^3$). The two purple prisms represent the electrodes whose designs are derived from the shapes of the surgical forceps' jaws (Fig. 2(D)). The electrodes are inserted into the tissue with a depth d and a distance L between two electrodes.

In the simulation, L was set from 2 to 8 mm with a step of 2 mm, and d was set from 0 to 4 mm with a step of 1 mm. Previous studies indicate that $\hat{\varepsilon}$ can increase with tissue compression [10, 11]. However, in our case, the tissue samples are thicker (20 mm) and the pressing displacement is small ($\leq$4 mm), corresponding to a small compression rate ($\leq$20%). Therefore, the increment of $\hat{\varepsilon}$ would be less than 10% during the tissue compression according to the above studies. The change of $\hat{\varepsilon}$ is neglected in this study since the impact from the change of E during the pressing of forceps, which will be illustrated later, is much greater. Considering the modeling described in Section II.A, we set the conductivity to σ_0 S/m and permittivity ε' of the tissue to be 0. Therefore, $|\omega\hat{\varepsilon}|$ is equal to σ_0. This simplification enables the FE simulation to be done using DC voltage, but does not affect the accuracy of the results.

The software package ANSYS Multiphysics was used for running the simulation. The results demonstrated that $|Z|$ decreased when d was bigger and L was smaller. The sensitivities of $|Z|$ to d and L were calculated: the sensitivity to d ranged from $449/\sigma_0$ Ω/mm to $24.2/\sigma_0$ Ω/mm, and the sen-

sitivity to L was from $31.8/\sigma_0\,\Omega$/mm to $6.3/\sigma_0\,\Omega$/mm. The higher sensitivity was found for the smaller value of L and d.

Based on the simulation results, we propose to measure $|Z|$ of the touching tissue with a specific jaw opening distance L and a flexible pressing depth d within a range from 2 to 4 mm during the application. This design considers that $|Z|$ is very sensitive to d, and in actual use it is difficult to obtain an accurate d since the measured organ can be moving due to physiological motions. In contrast, since L can be easily controlled by the surgical robotic system and this value has relatively low influence to $|Z|$, this parameter is controlled to be a specific value. Also, the range of d is set to be from 2 to 4 mm because when the tool tip barely touches the tissue (d = 0 and 1 mm) the tool tips may have unstable contact with the tissue, while when the forceps is pressing too deeply ($d > 4$mm) complications due to large tissue deformations and the change of tissue electric property can be involved.

C. Experimental evaluation with ex-vivo porcine tissues

Ex-vivo experiments were conducted to evaluate the proposed sensing method for tissue identification. A prototype of EBI sensor was made for the experiments as shown in Fig. 3(A). The EBI sensor consists of an electrical impedance converter (AD5933, Analog Inc., USA) and a micro-controller (Atmega328P, Atmel Co., USA). It can be directly mounted on top of a daVinci endowrist instruments (Maryland bipolar forceps Ref. 400172), and connected to its proximal end for measuring the EBI of the tissue contacting its jaws using the electrification connections already integrated in the tool. The measured value is sent to a computer via USB. The peak-to-peak voltage of the EBI sensor is set to be 0.4 V in order to satisfy the international standard IEC 60601. In addition, the excitation frequency is set to be 100 kHz, allowing the system to classify most different tissue types according to Kalvoy *et al.* [3] and Gabriel *et al.* [12]. Then the EBI sensor was calibrated with several known resistors ranging from 786 Ω to 8.2 kΩ, which covers the range of EBI for most tissue types (please refer to Fig. 4). The error rate was found to be 0.59% in average, and the maximum error rate was found to be 1.2%.

The experimental setup for measuring the EBI of ex-vivo porcine tissues is shown in Fig. 3(B). Four tissue types were used including muscle, liver, kidney, and lung. The forceps with the EBI sensor was fixed to the 4^{th} stage of a micro-motion stage (Siskiyou Co., USA) for controlling its vertical movement. During the experiments, L was fixed to be one of the followings: 2, 4, 6, and 8 mm. The position of the forceps was firstly adjusted to just touch the tissue, and this position was initialized as $d = 0$. Then we controlled the forceps to move 4 mm downwards, and recorded $|Z|$ in every 1 mm. Five

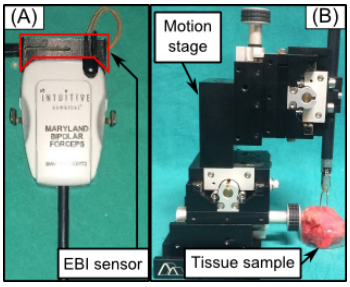

Fig. 3: (A)The prototype of the EBI sensing device; (B)The setup of the ex-vivo experiment.

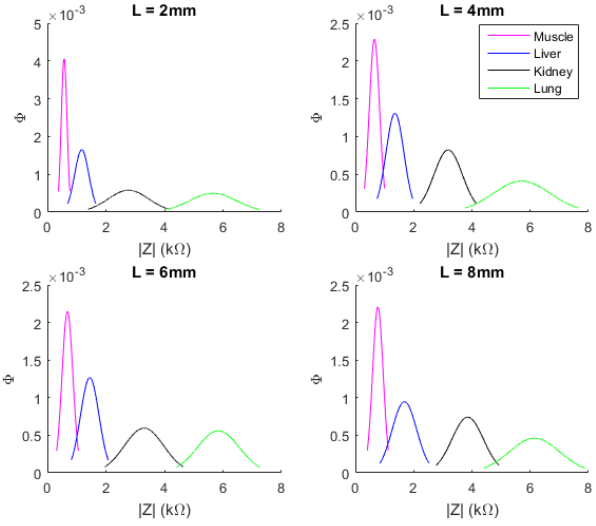

Fig. 4: The ex-vivo experimental results of four tissue types with different L and d = 2 to 4 mm.

samples were prepared for each tissue type, and 10 measurements were collected for different d and different L.

III. Results

For each tissue type Θ_i and a specific L_j, the experimental results with d = 2 to 4 mm were grouped as a class. All the classes were found to be normally distributed by the Kolmogorov-Smirnov test (all the p values are >0.05). Subsequently, the maximum likelihood estimation method was used to describe each class as $C_{ij} = N(\mu_{ij}, \sigma_{ij})$. Fig. 4 shows the Gaussian models with a width of 4 standard deviations of the mean in different L. In addition, the confusion matrix based on the $\pm 2\sigma$ Gaussian model was calculated and shown in Table 1. Each row of the matrix represents the tissue types determined by the EBI sensing system while each column represents the ground-truth tissue type. The confusion matrix indicates that the four tissue types can be classified with con-

Table 1: The confusion matrix: percentage of correctly classified tissue.

L=2 mm	muscle	liver	kidney	lung
muscle	100%	0	0	0
liver	7.18%	92.82%	0	0
kidney	0	3.14%	96.77%	0.09%
lung	0	0	0.59%	99.41%
L=4 mm	muscle	liver	kidney	lung
muscle	97.74%	2.26%	0	0
liver	6.56%	93.44%	0	0
kidney	0	0	99.95%	0.05%
lung	0	0	3.32%	96.68%
L=6 mm	muscle	liver	kidney	lung
muscle	98.03%	1.97%	0	0
liver	6.14%	93.86%	0	0
kidney	0	1.14%	97.89%	0.97%
lung	0	0	1.24%	98.76%
L=8 mm	muscle	liver	kidney	lung
muscle	99.24%	0.76%	0	0
liver	6.77%	93.23%	0	0
kidney	0	0	98.69%	1.31%
lung	0	0	4.31%	95.69%

siderably high accuracy ($\geq$92.82%) using the proposed EBI sensing method.

IV. Discussions

This study designed and assessed new technology to exploit EBI sensing on bipolar forceps for tissue identification. The confusion matrix for the classification of the four tissue types presented in Table 1 demonstrates that the sensing system can identify these tissue types with high accuracy.

In addition, the impact of two acquisition parameters, namely d and L, were investigated in this study. We proposed to measure $|Z|$ with a flexible d in a defined range (2 - 4 mm). This is because the EBI measurement is very sensitive to the parameter d according to the FE simulation in Section II.B. However, in practice, the pressing depth information is estimated by the kinematic information of the surgical robotic system, and this information may not be very accurate due to the limitation of the robot's encoder and the movement of the measured organ. In contrast, the proposed EBI measurement protocol requires the parameter L to be known, which can be obtained from the robotic system controller.

V. Conclusion

In this work we have presented an EBI measurement system that could be easily integrated in standard bipolar surgical tools for improving the sensing capabilities during RMIS procedures. The proposed system has been tested on ex-vivo animal tissue samples to evaluate its reliability. We have also identified the acquisition parameters that affect the EBI measurements obtained with a bipolar tool. The results confirm that the proposed system is able to repetitively recognize different types of tissue. Physical simulation has been performed to model the tool-tissue interaction, and the simulation results were confirmed by the experimental ones. Future work will focus on a more accurate FE simulation model involving tissue deformation during forceps pressing on the tissue. In addition, the electrical impedance will be measured in multiple frequencies for improving the detection accuracy. Also, the system will change to use current source for signal excitation in order to eliminate issues with contact impedance and guarantee a safer measurement.

Acknowledgements

This study has been partially supported by the ARS project (Grant No. H2020-ERC2017-3).

References

1. Pavan N, Zargar H, Sanchez-Salas R, et al. Robot-assisted versus standard laparoscopy for simple prostatectomy: multicenter comparative outcomes *Urology.* 2016;91:104–110.
2. Moccia S, Wirkert S J, Kenngott H, et al. Uncertainty-aware organ classification for surgical data science applications in laparoscopy *IEEE Transactions on Biomedical Engineering.* 2018.
3. Kalvøy H, Frich L, Grimnes S, Martinsen Ø G, Hol P K, Stubhaug A. Impedance-based tissue discrimination for needle guidance *Physiological measurement.* 2009;30:129.
4. Cheng Z, Davies BL, Caldwell DG, Mattos LS. A New Venous Entry Detection Method Based on Electrical Bio-impedance Sensing. *Annals of biomedical engineering.* 2018.
5. Cheng Z, Davies BL, Caldwell DG, Mattos LS. A venipuncture detection system for robot-assisted intravenous catheterization in *Biomedical Robotics and Biomechatronics (BioRob), 2016 6th IEEE International Conference on*:80–86IEEE 2016.
6. Laufer S, Ivorra A, Reuter V E, Rubinsky B, Solomon S B. Electrical impedance characterization of normal and cancerous human hepatic tissue *Physiological measurement.* 2010;31:995.
7. Zou Y, Guo Z. A review of electrical impedance techniques for breast cancer detection *Medical engineering & physics.* 2003;25:79–90.
8. Aberg P, Nicander I, Hansson J, Geladi P, Holmgren U, Ollmar S. Skin cancer identification using multifrequency electrical impedance-a potential screening tool *IEEE transactions on biomedical engineering.* 2004;51:2097–2102.
9. Martinsen O G, Grimnes S. *Bioimpedance and bioelectricity basics*. Academic press 2011.
10. Moqadam S M, Grewal P, Shokoufi M, Golnaraghi F. Compression-dependency of soft tissue bioimpedance for in-vivo and in-vitro tissue testing *Journal of Electrical Bioimpedance.* 2015;6:22–32.
11. Dodde RE, Bull JL, Shih AJ. Bioimpedance of soft tissue under compression *Physiological measurement.* 2012;33:1095.
12. Gabriel S, Lau RW, Gabriel C. The dielectric properties of biological tissues: III. Parametric models for the dielectric spectrum of tissues *Physics in Medicine & Biology.* 1996;41:2271.